

Ca depletion and the presence of dust in large scale nebulosities in radiogalaxies (II)^{*}

M.Villar-Martín^{1,2} and L.Binette³

¹ ST-ECF, Karl-Schwarzschild-Str 2, D-85748 Garching, Germany

² Dept. of Physics, University of Sheffield, Sheffield S3 7RH, UK

³ European Southern Observatory, Casilla 19001, Santiago 19, Chile (LBinette@eso.org)

Abstract. We investigate here the origin of the gas observed in extended emission line regions surrounding AGNs. We use the technique of calcium depletion as a test to prove or disprove the existence of dust in such a gas in order to discriminate between two main theories: (1) a cooling process from a hotter X-ray emitting phase surrounding the galaxy, (2) merging or tidal interaction between two or more components. We have obtained long slit spectroscopy of a sample of objects representative of different galaxy types although our main interest focus on radio galaxies. The spectral range was set to always include the [CaII] $\lambda\lambda 7291,7324$ doublet. The faintness or absence of such lines is interpreted as due to the depletion of calcium onto the dust grains and, therefore, is a proof of the existence of dust mixed with the gas in the EELRs.

1. Introduction

Extended emission surrounding AGNs has been detected in many active galaxies. Such structures have spatial scales that vary from 1kpc to hundreds of kpc. Many of the extended emission line regions (EELRs) are found in elliptical galaxies which are not gas rich objects, thus: where does the gas come from? Does it come from stellar evolution as a consequence of stellar winds and SN explosions? Or, on the contrary, is the origin external, and the gas is accreted from a companion galaxy rich in gas or from a hot halo surrounding the galaxy? In Paper I (Villar-Martín & Binette 1996) we made a review of the observational evidences which supports or contradict these theories, being an external origin easier to reconcile with the

Send offprint requests to: M. Villar-Martín, Dept. of Physics, University of Sheffield, Sheffield S3 7RH, UK

^{*} Based on observations carried out at the European Southern Observatory (ESO, La Silla, Chile)

observations. The morphological similarities with the systems of filaments surrounding galaxies near the centers of rich clusters suggests that the origin of the EELR result from cooling of the hot gaseous halos which surrounds the central galaxies. On the other hand, morphological and kinematical studies of the gas often suggest the existence of a collision or merger in the recent past.

The existence or not of dust mixed with the emitting gas has direct implications about the most plausible scenario for the formation of these extended ionized structures. In the scheme of the cooling flow theory, the hard intracluster radiation field would prevent dust from forming. If the material consists of galactic debris, the dust/gas ratio is expected to have a value appropriate to the chemical composition of a normal galaxy. Our aim is to check if the dust does exist in EELRs.

Ferland (1993) has proposed that the absence of the forbidden [CaII] lines $\lambda\lambda 7291,7324$ (F1 and F2 hereafter) can be used to infer the presence of dust mixed with the gas in the Narrow Line Region (see also Kingdon, Ferland & Feibelman, 1995). Calcium is very sensitive to dust. It suffers strong depletion into the dust grains and therefore, its abundance in the gaseous phase (responsible of the line emission) is lower than in a dust free nebula. The line emission should be fainter than expected, or even undetectable.

In Paper I, we proved that such test remains valid (and is very sensitive) under the conditions of the EELRs studied here. We studied in detail all the most plausible *alternative* mechanisms to that of internal dust for explaining the absence of [CaII] lines. No acceptable alternative solution was found and we concluded in favour of the validity of the method initially proposed by Ferland (1993). The observational results and their interpretation are presented in this paper. We have applied this test to a sample of objects of different types: radiogalaxies with extended emission line regions, cooling flows and starburst galaxies. Our main interest concerns to the EELR in radio galaxies.

Table 1. Observing Log

Name	RA(1950)	Dec(1950)	z	Comment	Exp time (s)	PA
NGC1052	02 38 37.33	-08 28 09	0.005	Liner	1800	270°
NGC6215	16 46 47.0	-58 54 30	0.005	Liner	2700	240°
NGC7552	23 13 25.0	-42 51 24	0.005	Liner	1200	270°
NGC7714	23 33 40.59	01 52 42	0.009	Starburst	2700	270°
PKS1404-267 (nuc)	14 04 38	-26 46 51	0.021	RG	2700	270°
PKS1404-267 (5" S)					2700	270°
PKS2014-55	20 14 06	-55 48 52	0.061	RG	3600	190°
PKS2152-69 (nuc)	21 52 58	-69 55 40	0.028	RG	2700	270°
PKS2152-69 (cloud)					3600	290°
PKS2158-380	21 58 17	-38 00 51	0.033	RG	2700	270°
PKS2356-61	23 56 29	-61 11 42	0.096	RG	3300	285°
PKS2300-18	23 00 23	-18 57 36	0.129	RG	2700	240°
2A 0335+096	03 35 52	09 48 10	0.035	CF	5400	147°
A2029	15 08 30	05 57 00	0.077	CF	2700	270°
A2597	23 22 42	-12 23 00	0.085	CF+RG	2700	197°

We describe the observations, data reduction and analysis of the spectra in section 2. In section 3 we present the results of the comparison between measurements and model predictions. A detailed analysis of the nuclear spectra is presented in section 4 and conclusions compose section 5.

2. Observations and data reduction

The observations were carried out on the nights 21-23 August on 1993. All the spectra were obtained at La Silla Observatory, Chile, with the 3.6 m telescope, using the EFOSC 1 spectrograph with a CCD detector (TEK#26) of 512×512 pixels² of $27 \mu\text{m}^2$. The slit width was $1.5''$. The grism used was, R150, with a dispersion of $120 \text{ \AA} / \text{mm}$, a wavelength bin of $3.3 \text{ \AA} / \text{pixel}$ and covering a spectral range of $\sim 6870\text{-}8560 \text{ \AA}$. The observing conditions were photometric. Table 1 gives a log of the observations.

2.1. Basic data reduction

The reduction of the data was done using standard methods provided in IRAF. The spectra were bias subtracted and divided by a flat-field frame (dome flat-field). Illumination corrections along the slit were found to be negligible.

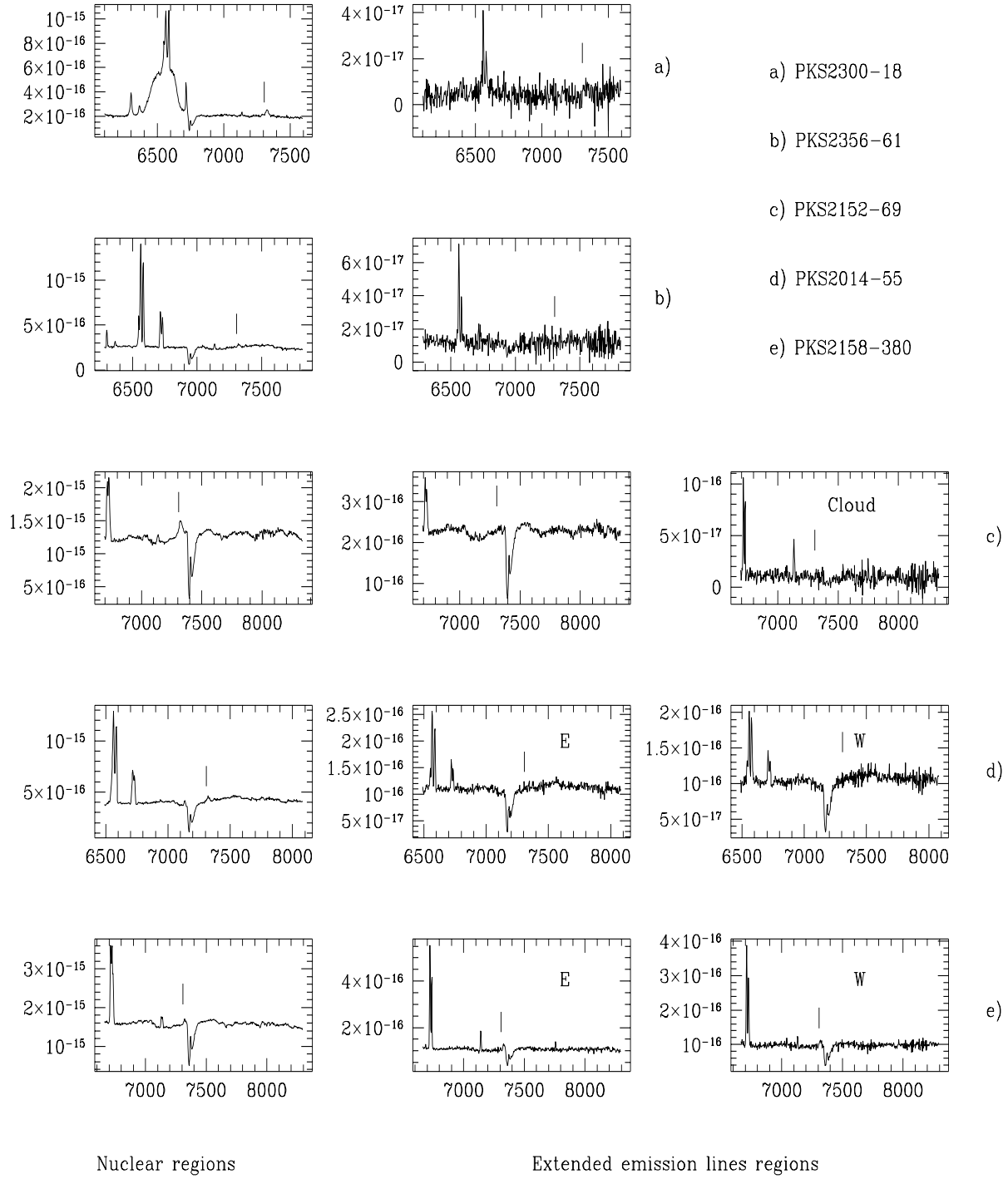
In general, we obtained three frames for each object and each slit position, allowing the direct removal of cosmic ray events. For a given object, all the frames corresponding to the same slit position were averaged together. In the cases where only two frames were available, the cosmic rays were removed visually, replacing the affected pixels by the mean of the surrounding region. The spectra were calibrated in wavelength using comparison spectra of an HeAr arc taken at the beginning and end of each night, and additionally before and after each object. The wavelength calibration was done very carefully in order to later

subtract the sky as accurately as possible. The IRAF routine “background” was used to subtract the contribution of the sky by interpolation of the background detected in windows close to and on both sides of the object. Using this method, the sky features were successfully subtracted.

2.2. Atmospheric extinction

The spectra were corrected for atmospheric extinction with the aid of mean extinction coefficients for La Silla. Molecular absorption bands of O_2 (the A band at 7620 \AA and the H_2O bands, bands in the region $7100\text{-}7450 \text{ \AA}$ and $8100\text{-}8400 \text{ \AA}$) were also evident in the spectra. They were removed separately from all the observed spectra. These absorption bands are composed of many closely spaced absorption features, unresolved in our spectra. Many of the features which comprise the A band are optically thick and therefore nearly independent of zenith distance, but most of those in the H_2O bands are not independent of time and zenith distance. In principle, the best method to remove these lines is to observe standard stars as close as possible in zenith distance and in time to that of the program object in order to obtain the best correction (c.f. Osterbrock, Shaw & Veilleux 1990). But as these authors pointed out, the star closest to the objects’s observing time and zenith distance is not always the one producing the best correcting spectrum.

The procedure we used was the following: we observed three different standard stars whose frames were reduced in the same way as described before. After modeling the atmospheric bands with them, we found that the best results were obtained with Feige 110, a dwarf with no intrinsic absorption features in the spectral range observed. A 1-dimensional integrated spectrum of the standard star was obtained by adding all the light along the spatial direction. A smooth fit to the continuum was done and then the original spectrum was divided by the fit. The result

**Fig. 1.**

Spectra of observed Radiogalaxies, nuclear (first column) and extended emission line regions (second and third columns). The expected position of the F1 line is indicated with |. Flux is given in units of $\text{erg s}^{-1} \text{cm}^{-2} \text{\AA}^{-1}$.

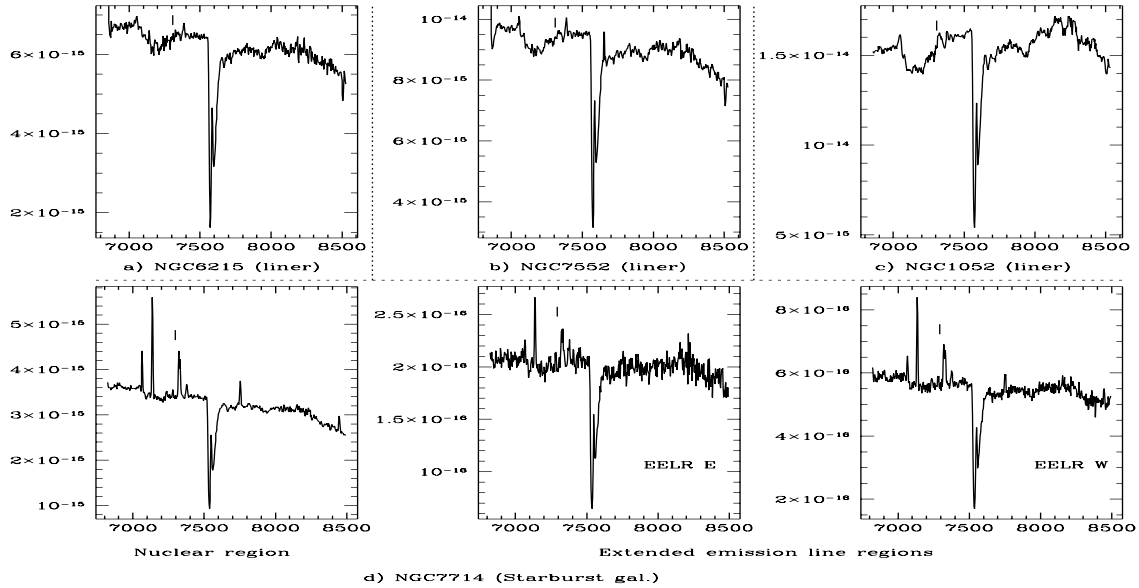


Fig. 2.

Spectra of observed Liners and Seyfert 2 galaxies. The liner spectra have been extracted from the whole spatial extension of the object. The expected position of the F1 line is indicated with | . Flux is given in units of $\text{erg s}^{-1} \text{cm}^{-2} \text{\AA}^{-1}$.

was a normalized spectrum which kept the features due to atmospheric absorption. Due to the dependence on zenith distance and time, we had to model the bands for each object, i.e. to construct a specific restoring spectrum for each object, multiplying the normalized spectrum by the appropriate factors.

2.3. Flux calibration

The atmospherically corrected spectra of the standard stars were used to obtain the flux calibration. For each night, we built a mean response curve from the two standard stars observed that night.

2.4. Template galaxy subtraction

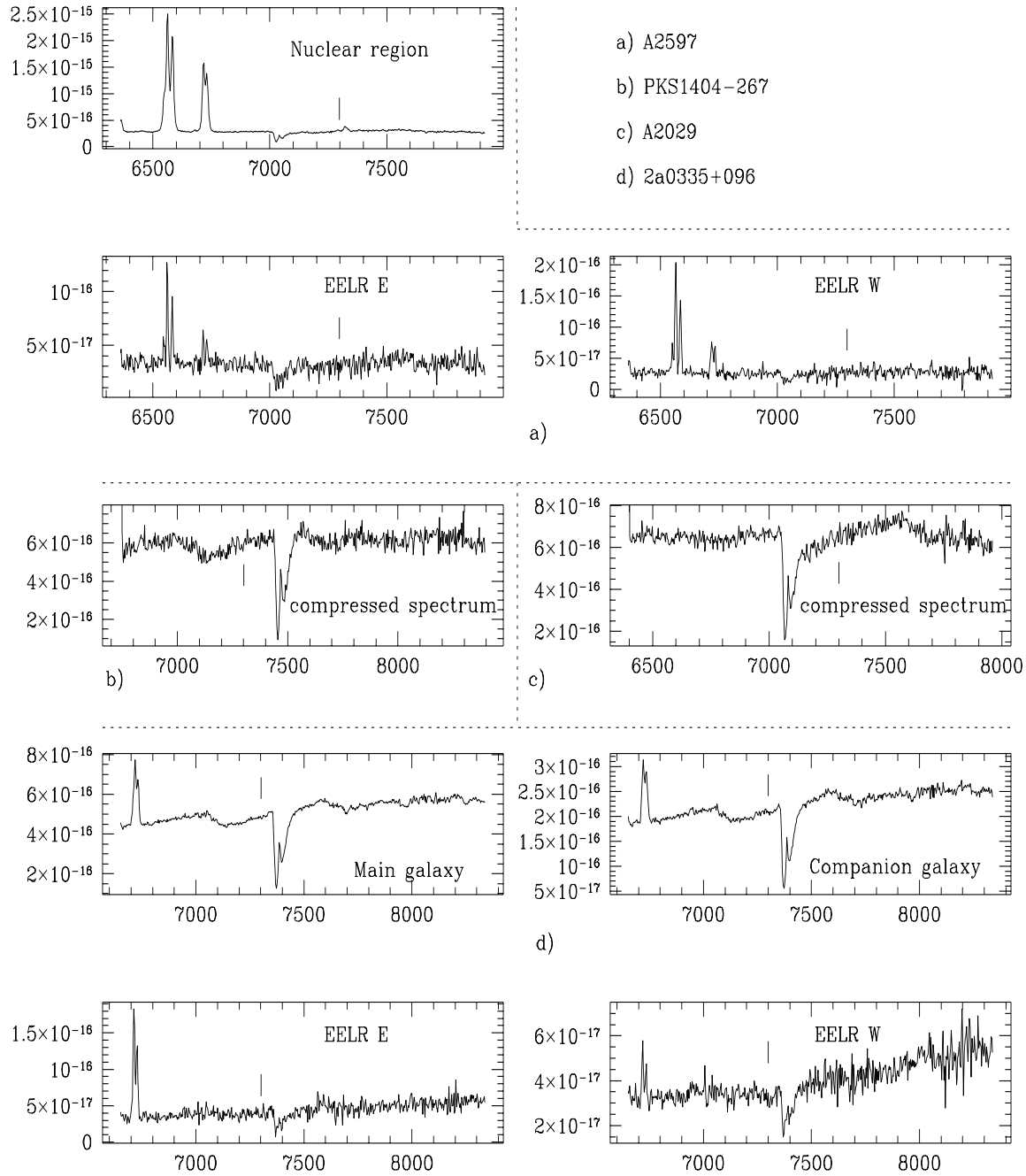
We checked that effects of stellar absorption features intrinsic to the galaxy could be neglected: the calcium doublet is on top of the raising part of a molecular band whose narrow line components are not resolved. Its only effect is to change the slope of the continuum under the doublet and we can easily correct for this effect, fitting a smooth continuum of appropriate slope in such region. $\text{H}\alpha$, a line which has been used as a reference in our prediction of the F1 line flux, can be underestimated due to the underlying $\text{H}\alpha$ absorption line. However, in our objects the $\text{H}\alpha$ emission is so strong that the difference is less than 5% of the emitted flux. This was estimated by comparing the EW of the emission line in our objects with the EW of the absorption feature from a template elliptical galaxy.

2.5. Data analysis

2.5.1. Extraction of the spectra

For those objects for which no extended emission lines were detected, we compressed the whole spatial extension in order to extract a 1-dimensional spectrum. For those objects showing extended emission lines, we separated it into two different components: the nucleus, and the extended emission line spectrum. In order to achieve this, we subtracted from the spatial profile of the brightest spectral line, the spatial profile from the nearby continuum. In this way, we are left with the spatial profile of the line emitting regions. In some cases, emission blobs appear well detached from the nuclear emission. In other cases, however, the extended and nuclear emission joined smoothly. In order to avoid contamination of the EELRs by the unresolved nuclear spectrum, we fitted a Gaussian (PSF) to the nuclear region. The residuals after subtracting this Gaussian were considered to pertain to the EELR. The resulting spectra are shown in Figs. 1, 2 and 3.

It is possible that we may be venturing close enough to the nucleus to sample higher densities, more typical of the classical narrow line region (with densities higher than 10^3 cm^{-3}). To verify this, when it was possible, we used the [SII] doublet to estimate the density. The values were always below 100 cm^{-3} , which indicates that the spectra are dominated by low density gas. In any event, even if the NLR dominated the emission, calculations show that at high densities the line F1 (in the dustfree case) if any-

**Fig. 3.**

Spectra of objects with properties associated with cooling flows. The spectra of PKS1404-267 and A2029 have been extracted from the whole spatial extension of the object. The expected position of the F1 line is indicated with |. Flux is given in units of $\text{erg s}^{-1} \text{cm}^{-2} \text{\AA}^{-1}$.

thing becomes stronger than many other lines as a result of its very high critical density and of the increase in electronic temperature. Our conclusions about inferring dust or not are therefore not affected by nuclear contamination. (Higher density models would in fact imply a stronger calcium depletion).

2.5.2. Line measurements

IRAF routines were used to measure the emission line fluxes. For the blends, decomposition procedures were used, fitting several Gaussians at the expected positions of the components. The fluxes correspond to the values derived from the sum of Gaussians which better fitted the profile.

The upper limits on [CaII] emission were measured directly from the noise level in the data.

3. Observed and predicted F1 fluxes

3.1. Prediction of F1 fluxes

The second component of the [CaII] doublet (F2) is the weakest and is blended with the [OII] $\lambda\lambda$ 7320,7330 multiplet. The first component is the strongest and lies well aside, some 30 Å shortward of [OII]. It is straightforward to isolate it given a reasonable spectral resolution. Therefore, for simplicity, we have based our study on the measurement of this line. The observed values are compared with the flux that photoionization models predict. MAPPINGS (Binette et al. 1993a,b) is the multipurpose photoionization-shock code which we used for the modeling. It considers the effects of dust mixed with the ionized gas: extinction of the ionizing continuum and of the emission lines, scattering by the dust, heating by dust photoionization and depletion of heavy elements. The appropriate input parameters for the models are justified in Paper I.

The predicted value of the F1 flux has been computed in the following way: we used as reference line (*ref line*), the strongest and/or the easiest line to measure, like H α , [SII] $\lambda\lambda$ 6716,6731, the [OII] $\lambda\lambda$ 7320,7330 blend and/or [ArIII] λ 7136. The appropriate photoionization model allows the prediction of $R = \frac{F1}{\text{ref. line}}$, from which we can easily deduct the F1 flux:

Predicted F1 flux = $R \times$ *Measured flux in the reference line*.

In Table 2, we show for each object and for each spatial region the reference lines used, the measured flux, the predicted $R = \frac{F1}{\text{ref. line}}$ ratio, the measured F1 flux and its theoretical value. For the nuclear regions, we always base our predictions on the blend [OII] $\lambda\lambda$ 7320,7330 as reference line. The density in the nuclear narrow line region spans a wide range up to 10^6 cm^{-3} . The critical density of the [CaII] forbidden lines is very high, and the flux of the lines under the nuclear conditions are predicted to be far stronger than the [OII] lines (Ferland 1993). The

low critical density [OII] line can be de-excited as a result of the high nuclear density so that if [CaII] remains much smaller than [OII], it is actually a more stringent test since high densities would have actually helped to increase the [CaII]/[OII] ratio. To measure the flux in the [OII] blend, we assume that there is a negligible contribution from the F2 component. This assumption is reasonable: it is fainter than F1 and, in any event, it is near or under the detection limit in all cases. We can therefore assume that the [OII] multiplet is not contaminated by F2.

3.2. Comparison with observations

The comparison between the measured and predicted F1 flux values shown in table 2 demonstrates that, whenever the calculations were possible (sometimes, however, there was not any reference line available), it is always fainter (non detected in most cases) than expected. This result is common to all the regions considered here: nuclear, EELRs and cooling flow filaments. It demonstrates that calcium is depleted and, therefore, *the gas is mixed with dust*, both in the nuclear as well as in the extended emitting gas in radio galaxies and cooling flow filaments.

Donahue & Voit applied this same test to the emission line nebulae in cluster cooling flows (1993). They interpreted the observed lack of [CaII] emission as depletion within the ionized filaments of calcium onto dust grains. Although for quite a different sample of objects, our work support these results, namely that the *ionized gas* which emits the low excitation lines observed in nuclear regions of AGNs, in large scale ionized gas in RGs, and in the filaments in objects classified as ‘cooling flows’ must all contain dust.

The most important result is the confirmation that *dust exists mixed with the ISM in low z radio galaxies*.

4. Discussion

4.1. Implications on the origin of the gas

As explained in Paper I, there are some pieces of evidence indicative of dust *in the extended ionized gas* in active galaxies, mainly derived from polarization measurements, which show the existence of scattered nuclear light over large spatial scales, although it is difficult to discriminate between dust and electrons as the scattering agent. Our results confirm that dust exists *mixed with the ISM in low redshift radio galaxies*.

As mentioned before, this produces discrepancies with the traditional cooling flow theory, which would now be required to explain the formation of dust in a shorter time than the cooling time! According to this theory (see Fabian 1994 for a review), the galaxies, groups and clusters of galaxies were formed out of gas that collapsed gravitationally. During this process, gravitational energy was released which heated the clouds and a hot X-ray atmosphere resulted. Inhomogeneities in the gas cause matter

Table 2. Emission line fluxes for the observed sample of galaxies (in units of $\text{erg s}^{-1} \text{cm}^{-2} \text{\AA}^{-1}$). The superscripts M and P indicate measured and predicted values respectively. The last two columns show the predicted and measured values for the $F1$ line. For those objects where the calculations were possible, the observed line is clearly fainter than predicted by photoionization models.

Name	Spatial reg.	ref line	$Flux^M$	$\frac{F1}{ref\ line}^P$	$Flux(F1)^P$	$Flux(F1)^M$
NGC1052	Total	None	—	—	—	$\leq 6.99\text{e-16}$
NGC6215	Total	None	—	—	—	$\leq 3.34\text{e-16}$
NGC7552	Total	None	—	—	—	$\leq 3.95\text{e-16}$
NGC7714	Total	[OII] λ 7325	1.59e-14	≥ 1.00	$\geq 1.59\text{e-14}$	$\leq 6.84\text{e-17}$
PKS1404-267	Nucleus	None	—	—	—	$\leq 1.79\text{e-16}$
	5" South	None	—	—	—	$\leq 5.23\text{e-17}$
PKS2014-55	Nucleus	[OII] λ 7325	1.54e-15	≥ 1.00	$\geq 1.54\text{e-15}$	$\leq 3.34\text{e-17}$
	EELR (E)	H α	1.47e-15	~ 0.45	6.62e-16	$\leq 2.60\text{e-17}$
	EELR (W)	H α	1.06e-15	~ 0.45	4.77e-16	$\leq 3.18\text{e-17}$
PKS2152-69	Nucleus	[OII] λ 7325	7.48e-15	≥ 1.00	$\geq 7.48\text{e-15}$	1.92e-16
	EELR	[SII] λ 6731	1.33e-15	~ 0.40	5.32e-16	$\leq 3.03\text{e-17}$
	Cloud	[ArIII] λ 7136	3.86e-16	~ 4.50	1.74e-15	$\leq 2.24\text{e-17}$
PKS2158-380	Nucleus	[OII] λ 7325	4.03e-15	≥ 1.00	$\geq 4.03\text{e-15}$	3.15e-16
	EELR (E)	[ArIII] λ 7136	7.28e-16	~ 5.0	3.64e-15	$\leq 2.55\text{e-17}$
	EELR (W)	[ArIII] λ 7136	3.00e-16	~ 5.0	1.5e-15	$\leq 5.00\text{e-17}$
PKS2356-61	Nucleus	[OII] λ 7325	9.39e-16	≥ 1.00	$\geq 9.39\text{e-16}$	2.78e-16
	EELR	H α	5.36e-16	~ 0.18	9.6e-16	$\leq 1.03\text{e-17}$
PKS2300-18	Nucleus	[OII] λ 7325	1.80e-15	≥ 1.00	$\geq 1.80\text{e-15}$	4.37e-16
	EELR	H α	3.61e-16	~ 0.40	1.44e-16	$\leq 1.97\text{e-17}$
2A 0335+096	cD galaxy	[SII] λ 6725	7.46e-16	~ 0.40	2.98e-16	$\leq 2.72\text{e-17}$
	EELR (E)	[SII] λ 6725	2.24e-15	~ 0.40	8.96e-16	$\leq 1.29\text{e-17}$
	EELR (W)	[SII] λ 6725	4.22e-16	~ 0.40	1.68e-16	$\leq 1.40\text{e-17}$
	companion	[SII] λ 6725	7.89e-15	~ 0.40	3.16e-15	$\leq 1.69\text{e-17}$
A2029	Total	None	—	—	—	$\leq 1.43\text{e-16}$
A2597	Nucleus	[OII] λ 7325	1.79e-15	≥ 1.00	$\geq 1.79\text{e-15}$	5.14e-16
	EELR	H α	2.32e-15	~ 0.50	1.16e-15	$\leq 5.86\text{e-17}$

from the hot atmosphere to cool down and fall towards the center of the galaxy or cluster. In this picture, the resulting filaments would eventually become visible at optical wavelengths and would emit strong lines. For massive galaxies and cluster, the cooling process would have been slower than for normal galaxies and the hot atmosphere would still exist, with typical temperatures of several million K, and be emitting strongly in the X-ray band.

If this is actually the origin of the gas in the EELRs (and cooling flow filaments), it should clearly be devoid of dust. Any dust introduced in the hot intracluster medium would be sputtered and rapidly destroyed (time scale of the order of 10^7 years) (Draine & Salpeter 1979), much before the filaments cooled down and became visible. Is there a way to introduce dust in the filaments during the cooling process? The common place where dust is formed is stellar atmospheres. Do stars exist in the accreted gas? Such gas must be deposited in some form and it has been generally thought that the more plausible fate for most of the gas is the formation of new stars (e.g., O’Connell & McNamara 1989; Fabian, Nulsen & Canizares 1991).

Although there are some indications of star formation in cooling flow galaxies, the latter seems to be taking place in the inner parts (over the central few kpc) (Cardiel, Gorgas & Arag3n-Salamanca 1995; Fabian 1994). There is a lack of evidence of star formation (or any kind of stars) at large distances, out of the main body of the galaxies, where the EELRs filaments are still visible.

In high z RGs, there is an extended blue continuum aligned with the radio axis which has often been interpreted as due to young stars. However, as I mentioned already before, further results (e.g., Tadhunter, Fosbury & di Serego 1988; Cimatti et al. 1993) proved that this continuum is polarized and that the contribution of a hidden quasar continuum scattered by dust and/or electrons in the ISM constitutes very likely an important component (in fact, this extended polarized UV continuum has been used as a proof of the existence of dust in the EELRs of high z radio galaxies). This effect has also been detected in some radio galaxies at low z (Cimatti & di Serego Alighieri S. 1995). Although young stars may exist, we don’t have a clear idea about their overall contribution.

There is another mechanism which can form dust: if most of the cooled gas from a flow does not form stars with normal IMF, maybe it remains as cold clouds or as low-mass stars. There are evidences of X-ray absorption (White et al. 1991; Mushotzky 1992; Allen et al. 1993) in cooling flows in cluster of galaxies. The absorbing material could be in the form of cold gas embedded in the hot intracluster medium of the cooling flow (White et al. 1991; Daines, Fabian & Thomas 1994). This cold gas, very slightly photoionized by X-rays from the surrounding hot corona, can become molecular (Ferland, Fabian & Johnstone, 1994). Fabian, Nulsen & Canizares (1994) propose that the conditions suitable for dust to form may occur in this cool gas, through the condensation of gaseous particles. The authors propose that the gas which is cooling towards the center could be a mixture of both the molecular gas and the very hot gas and, therefore, could contain the existing dust. However, even if such a scheme was possible, the dust grains will not remove the calcium which already existed in the hot gas; the temperature is too high for the condensation of calcium onto the dust grains. Therefore, we should observe the CaII lines from the hot gas when it cools down, even if it contains dust.

On the other hand, the interaction scenario (gas accreted from outside the galaxy, as a result of recent tidal interactions or mergers between two or more components) predicts the existence of dust mixed with the gas, the one already existing in the interacting objects. Some morphological evidences and theoretical ideas (see Paper I) support this scene. Heckman et al. (1986) showed that a large fraction of powerful radio galaxies have morphological features (shells, tails, loops, etc) similar to those produced in numerical simulations of galaxy interactions (e.g., Toomre and Toomre 1972; Quinn 1984). Kinematic measurements show that the radio galaxy EELR generally have a high specific angular momentum which is difficult to reconcile with the cooling flow picture (Tadhunter, Fosbury & Quinn 1989).

Therefore, if there is a common origin for the EELRs of all radio galaxies, our results suggest that it is mergers or tidal interactions. However, we don't exclude the possibility of an origin which is *not* universal, that is, which may differ from object to object.

5. Conclusions

We have confirmed that the gas in extended emission line regions in radio galaxies at low z is mixed with dust.

Our results support the existence of dust mixed with the gas in the Narrow Line Region and in the cooling flow filaments.

If there is an universal origin for the EELRs, the existence of internal dust favours mergers or tidal interactions as the most plausible scenario.

Acknowledgements. MV-M acknowledges support from the Deutsche Forschungsgemeinschaft; also thanks to A. Caulet,

R.A.E. Fosbury, J. van Loon, R. Pelletier and I. Pérez-Fournón for useful discussions.

References

- Allen S.W., Fabian A.C., Johnstone R.M., White D.A., Daines S.J., Edge A.C., Stewart G.C., 1993, MNRAS, 262, 901
 Binette L., Magris C.M., Martin P.G., 1993a, *Ap&SS*, 205, 141
 Binette L., Wang J.C.L., Zuo L., Magris C.M., 1993b, AJ, 105, 797
 Cimatti A., di Serego Alighieri S., Fosbury R.A.E., Salvati M., Taylor D., 1993, MNRAS, 264, 421
 Cimatti A., di Serego Alighieri S., 1995, MNRAS, 273, L7
 Cardiel N., Gorgas J., Aragón-Salamanca A., 1995, MNRAS, 277, 502
 Daines S.J., Fabian A.C., Thomas P.A., 1994, MNRAS, 268, 1060
 Donahue, M., Voit G.M., 1993, ApJ, 414, L17
 Draine B.T., Salpeter E.E., 1979, ApJ, 231, 77
 Fabian A.C., Nulsen P.E.J., Canizares C.R., 1991, *ARA&A*, 2, 191
 Fabian A.C., 1994, *ARA&A*, 32, 277
 Ferland G.J., 1993, in Proc. Madrid Meeting on The Nearest Active Galaxies, ed. J.E. Beckman, H. Netzer & L. Colina, p. 75
 Ferland G.J., Fabian A.C., Johnstone R.M., 1994, MNRAS, 266, 399
 Heckman T.M., Baum S.A., van Breugel, W.J.M., Miley G.K., Illingworth G.D., Bothun G.D. & Balick B., 1986, ApJ, 311, 526
 Kingdon J., Ferland G.J., Fiebelman, W.A., 1995, ApJ, 439, 793
 Mushotzky R.F., 1992, in Fabian A.C., ed., Clusters and Superclusters of Galaxies. Kluwer, Dordrecht, p.91
 O'Connell R.W., McNamara B.R., 1989, AJ, 98, 2018
 Osterbrock D.E., Shaw R.A., Veilleux S., 1990, ApJ, 352, 561
 Quinn P.J., 1984, ApJ, 279, 256
 Tadhunter C.N., Fosbury R.A.E., di Serego Alighieri S., 1988, in Maraschi L., Maccacaro T. & Ulrich M.H., eds., "BL Lac Objects", Springer-Verlag, Berlin, p.79
 Tadhunter C.N., Fosbury R.A.E., Quinn P.J., 1989, MNRAS, 240, 255
 Toomre A., & Toomre J., 1972, ApJ, 178, 623
 Villar-Martín M., Binette L., 1996, A&A, in press
 White D.A., Fabian A.C., Johnstone R.M., Mushotzky R.F., Arnaud K.A., 1991, MNRAS, 252, 72